

Development and Validation of a Neck Muscle FE Model for Lateral Impact Simulation

Ronggui LU, Fan LI, Honggeng LI

*State key Laboratory of Advanced Design Manufacturing for Vehicle Body
Hunan University, Changsha 410082, China*

Abstract: Head-neck injury is one of the most common injuries found in vehicle accidents, especially in low-speed collisions. Neck muscle activation affects the dynamic response of head-neck significantly. The aim of the present paper was to develop and validate a neck muscle FE model with passive and active properties that can be used for occupant safety study in lateral impact accidents. The geometry model of neck muscle was reconstructed from MIR images of a fifty percentile male. The model was then combined with a previously developed and well-validated head-neck FE model by means of Kriging method. Passive and active behavior of a single neck muscle was defined by coupling Ogden and Hill material models. The neck muscle FE model was validated against 7g volunteer tests of lateral impact. The results showed that the responses of the neck muscle model were consistent with the test results and muscle activation response had great effects on the head-neck dynamic responses. And this model could be further used for biomechanical studies of occupant head-neck injury in lateral impact accidents.

Keywords: neck muscle model; muscle activation; lateral impact; dynamic responses

1 Introduction

Human head-neck injuries that often cause severe damage (both physical and mental) to people are common in traffic accidents, which lead to huge economic burden for the society^{[1][2]}. Many researches have been launched during the past years, but the mechanism still remains a lot to be studied. Experiments and numerical simulation are the two widely used ways to perform study, while experiments concerning human subjects are difficult to implement due to the ethical reasons. Also, the measuring methods are limited and the information acquired from experimental researches is rather insufficient. Thanks to the rapid development of computer technology, numerical simulation could well complement the experimental studies. Hence studies with human head-neck FE models established around.

To obtain kinematic responses of the head in frontal and lateral directions, Dauvilliers F et al. developed a human neck FE model with vertebrae and head considered as rigid parts, discs and different ligaments modeled by brick and spring elements^[3]. When determining the stiffness of the ligament, the passive property of the muscles were taken into account; Jost R et al. built a human head-neck model with bony vertebrae modeled by shell elements, muscles and ligaments modeled by membrane and spring-damper elements^[4]; Ejima firstly took the geometric shape and anatomical location into consideration and built a neck muscles model with detailed geometric shape^[5]; Frechede et al. and Meyer et al. developed a human head-neck FE model with solid element^{[6][7]}.

Human head-neck FE models with passive muscle properties only were inadequate to study the injury mechanism since the activation of neck muscles played an important driving role in head-neck kinematics investigation^[8]. Famous human head-neck FE model THUMS was developed by Iwamoto M. et al with both active and passive muscle properties as well as the detailed muscle geometry^{[9][10]}, which was used widely in studying injury mechanism resulting from vehicle-pedestrian collisions. Another famous human head neck FE model, GHBMC, was developed by FS Gayzik et al^[11], then the muscle activation dynamics was incorporated into this model by Feller L et al^[40]. The active muscles of both THUMS and GHBMC were simulated by beam elements that were modeled by MAT_156 material, an LS -

DYNA material model based on a Hill-type muscle model. The Hill-type element, consisted of contractile and discrete element paralleling to elastic springs and viscous dampers, was extensively used in the discrete models to model the active muscle property. MJ van der Horst et al. also used Hill-type element to simulate the activation of neck muscles in vehicle frontal, lateral and rear collision ^[12], which offered a detailed method of implementing muscle activation. Though several studies had produced estimates of muscle activation, the data still remained insufficient. In order to define the biofidelity and stability of the muscle with passive and active properties, Li F et al. conducted a research to study the methodology. In his work^[13], two kinds of coupled models, Hill elements coupled with hyper-elastic elements and Hill elements coupled with viscoelastic elements, were developed and analyzed for comparison. Rabbit TA tests conducted by Myers et al.^{[14][15]} were used to exhaustively evaluate the two models. Isometric contraction and axial compression were also simulated to evaluate the computational stability. The significant finding to emerge from this study ^[13] was that the coupled muscle models had good biofidelity and stability for the simulation of muscle activation. Both muscle models were able to fulfill the requirement of neck muscle system modeling for biomechanical study.

In the present study, the project was undertaken to develop a 3D human neck muscles FE model with passive and active muscle properties and integrated this model into HBM-Head-Neck FE model, then validated the whole combined model (New HBM-Head-Neck FE model) through volunteer tests by performing low-speed vehicle lateral collision simulations. The findings demonstrated that the New HBM-Head-Neck FE model had a good biofidelity and can be used for the future numerical research.

2 Method and Materials

In this paper, A detailed human neck muscles geometry model was developed from MRI and integrated into the HBM-Head-Neck FE model developed by Hunan University^[16].The combined model was validated through the volunteer tests in 7g lateral impact.

2.1 HBM-Head-Neck FE model

The HBM-Head-Neck FE model includes two parts: The HBM-Head-Neck Model II and the thorax model. The HBM-Head-Neck Model II, shown in Figure 1, was developed and validated by Yang JK and Wang F et al^[16]. This model represented a 50th percentile male and comprised seven cervical vertebrae with trabecular and bone tissues, skull base, facet joints with cartilage, cervical ligaments as well as intervertebral discs. The skull and the shoulder were considered rigid for boundary conditions and the muscle modeled by single beam element was removed. The thorax

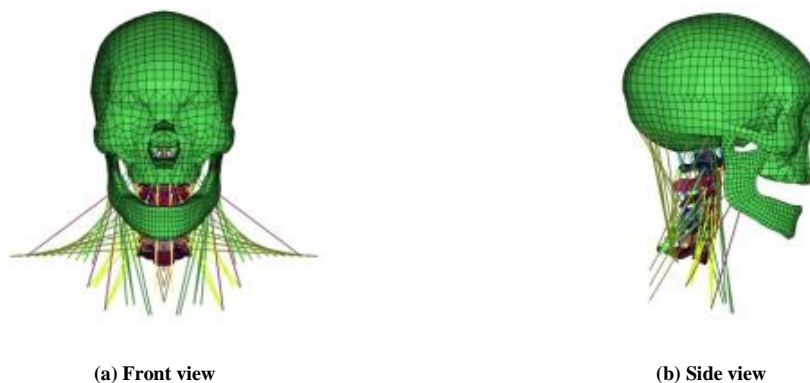


Figure 1. HBM-Head-Neck Model II

model connected with HBM-Head-Neck Model II, shown in Figure 2(a), was created and validated by Wang F et al.^{[20][21]}. The combined HBM-Head-Neck FE model, without muscle beam elements, was shown in Figure 2(b).



Figure 2. thorax model (a) and HBM-Head-Neck FE model (b)

2.2 Modeling of the Neck Muscles

2.2.1 Reconstruction of geometry model

The detailed geometry model of human neck muscles was developed from a 50th percentile adult male neck Magnetic Resonance Images (MRI) that were obtained from the joint research of Li F et al and Paris Institute of Technology^[22]. In the research, the necks of 16 healthy volunteers were scanned with 1.5T MRI scanner to get the neck MRI images. And the geometry models of neck muscles of 16 volunteers were reconstructed by Li Fan et al based on the deformation of a Parametric Specific Object (DPSO) method put forward by Jolivet et al.^[23]. Figure 3 shows the adult male neck MRI image and the geometry model of neck muscles. According to the equivalent principle, all the neck muscles were divided into 12 groups as follows: Infrahyoid muscles, Anterior cervical muscles, Levator muscle of scapula, Longissimus capitis, Musculi longissimus cervicis, Musculi sternocleidomastoideus, Small prismatic muscle,

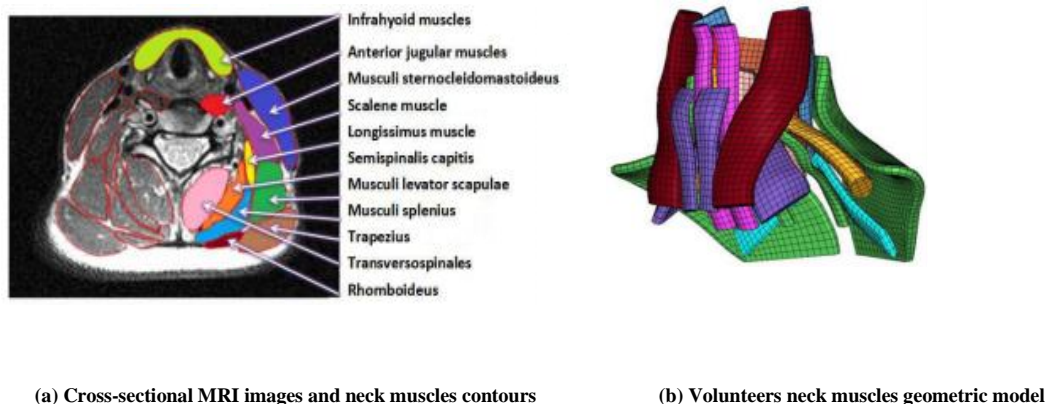


Figure 3. Neck cross-sectional MRI images and volunteers neck muscles geometric model

Transverse spine muscle, Semispinalis capitis, Splenius capitis muscle, Scalenus; Trapezius, Rectus capitis muscle, Musculus obliquus capitis simulated by one dimensional beam element. Regarding one single muscle, it consisted of three parts: the tendon modeled by beam element, the passive muscle belly modeled by solid element and the active

muscle modeled by beam element in series(see in Figure 4). Within the model, the active element was incorporated into the passive with shared nodes.

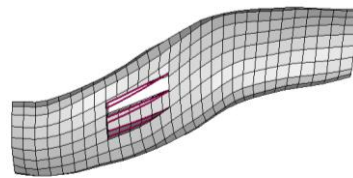


Figure 4. The coupled single muscle

The physiological cross sectional area (PCSA) of each muscle group in the axial plane and the muscle length was calculated, and the PCSA coupled with length values of the cervical muscles were compared with published data from PMHS studies ^[2], as can be seen in Table 1.

Table 1. The PCSA and length of cervical muscle model

Name	Length(mm)			PCSA(mm ²)	
	Goel	Kami	Li F	Van Ee	Li F
Hyoid muscles	-	-	95.2	130	133.6
Longissimus	-	-	160	300	184.9
levator scapulae	232	82	120.8	310	308.8
Longus capitis	376	-	93.2	250	73.9
Longus colli	268	-	167.8	250	63.4
Sternocleidomastoideus	192	190	162.5	490	558.4
Transverse spinalis	-	-	90.8	1360	1281.1
Semispinalis capitis	223	117	90.3	1360	246.9
Splenius	155	123	117	260	252
Scalenus	105	-	105.1	430	281
Trapezius	460	391	154	1370	1236.5

The geometry of neck muscles was integrated into the HBM-Head-Neck FE model with Kriging interpolation method after reconstruction^[13], and the New HBM-Head-Neck FE model was shown in Figure 5.

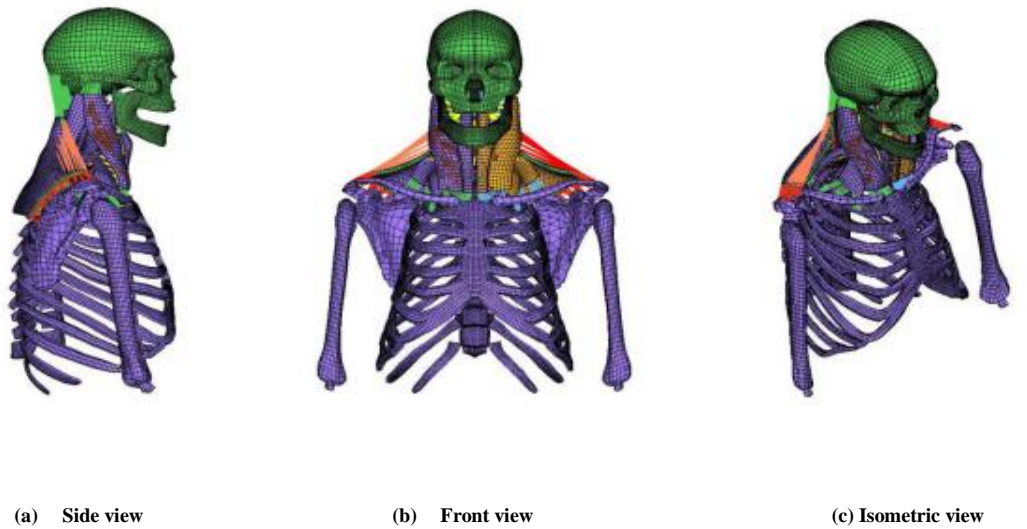


Figure 5. The New HBM Head-Neck FE model

2.2.2 Material modeling

Referring to the findings demonstrated experimentally by Li F et al.^[13], in his research, both of the muscle models, Hill elements coupled with hyper-elastic elements and Hill elements coupled with viscoelastic elements, obtained high biofidelity. The former was more stable and was thus adopted by our present study.

The activation of muscles were modeled by beam elements defined with Hill material. The active contracting force of each beam element (F_{ce}) is given by:

$$F_{ce} = A(t) F_l(l) F_v(v) F_{max} \quad (1)$$

Where $A(t)$ is the time history of muscle activation, $F_l(l)$ is the function of muscle force versus length, $F_v(v)$ is the function of muscle force versus contraction velocity, F_{max} is the maximum isometric contracting force. $F_v(v)$ and $F_l(l)$ used in the model were given in Figure 6. The parameters of Hill material (LS-DYNA keyword) were defined as in Table 3.

The F_{max} and V_{max} for every muscle model needs to be defined as:

$$F_{max} = \sigma_{max} \cdot PCSA \quad (2)$$

$$V_{max} = 10 l_{opt} \quad (3)$$

Where σ_{max} is the maximum isometric contraction stress, which was chosen $0.5Mpa$ according to the research of Winters and Stark^[27]. When isometric contraction stress reaches the its maximum, the length l_{opt} was chosen $1.05mm$ from the research of Zajac^[30]. The value of PCSA were measured in the neck muscles FE model. The active force was provided by several parallel Hill beam elements within a single muscle, leading to the result that the force should be

distributed by the beam element eventually. The number of Hill muscle model M and the peak isometric force F_{max} were shown in Table 2.

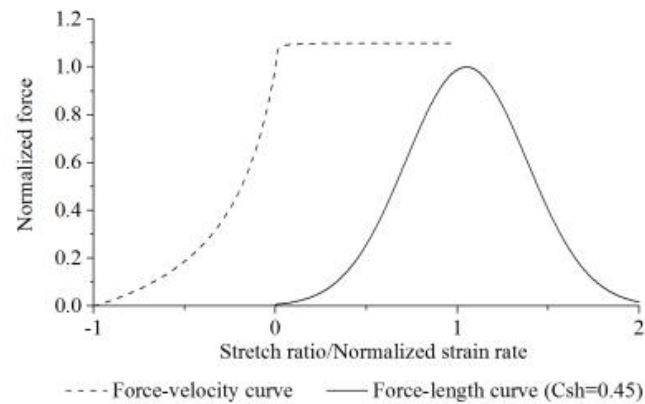


Figure 6. Force-length and Force-velocity curves of Hill muscle model

Table 2. The cervical muscles, number of Hill muscle model M and the peak isometric force F_{max}

Name	PCSA(mm ²)	F_{max} (N)	M	V_{max} (m/s)	F_{max} / M (N)
Infrahyoid muscles	133.6	66.8	6	0.99	11.1
Anterior cervical muscles	184.9	92.4	4	1.68	23.1
Levator muscle of scapula	308.8	154.4	8	1.27	19.3
Longissimus capitis	73.9	36.9	4	0.98	9.2
Musculi longissimus cervicis	63.4	31.7	1	1.76	31.7
Musculi sternocleidomastoideus	558.4	279.2	10	1.71	27.9
Transverse spine muscle	1281.1	640.5	6	0.95	106.8
Semispinalis capitis	246.9	123.4	10	0.94	12.3
Splenius capitis muscle	252.0	126.0	8	1.23	15.8
Scalenus	281.0	140.5	16	1.10	8.8
Trapezius	1236.5	618.3	40	1.62	15.5

Ogden material, normally used to simulate the soft tissue in biomechanical area, is generally considered to be fully incompressible since the bulk modulus greatly exceeds the shear modulus in magnitude^[31]. It is described by the energy potential in the following equation:

$$W = \sum_{i=1}^3 \sum_{j=1}^n \frac{\mu_j}{\alpha_j} (\lambda_i^{\alpha_j} - 1) + \frac{1}{2} K (J - 1)^2, \quad (4)$$

Where μ_j and α_j are constants to be determined, λ is the principal stretch, K is the bulk modulus and J is the Jacobian determinant. Ogden material is not a rate effective material. To simulate the strain rate, viscoelastic component should be added as following:

$$\sigma = \sigma^e + \sigma^v, \quad \sigma^v = \int_0^t G(t - \tau) \frac{\partial \sigma}{\partial \tau} d\tau, \quad (5)$$

Table 3. Main parameters of the Hill material and Ogden material. (Adapted from [13])

Name	Parameters	Value
Passive parameters for Ogden material	Density	1.06 (kg/m ³)
	Poisson's ratio	0.495
	Constants μ_i	μ_i (MPa) = 0.01148
	Constants α_i	α_i = 12.32
	Prony series	G_i (MPa) = 0.001;0.575;0.288;0.137 β_i (s ⁻¹) = 73.4;50.3;42.7;0.255
Active parameters for Hill material	Muscle specific maximum isometric force	$F_{max} = 22.5$ (N)
	Muscle optimal length factor to the rest length	$l_{opt}/l_{rest} = 1.05, l_{rest} = 1$
	Shape factor of the force-length curve	$C_{sh} = 0.45$
	Shape factor of the shortening curve	$C_{short} = 0.3$
	Shape factor of the lengthening curve	$C_{leng} = 0.005$
	Shape factor of the ratio of maximum isometric force during lengthening	$C_{mvl} = 1.1$
	Maximun isometric speed	$V_{max} = 0.945$ (m/s)
Tendon	Young's modulus	1.2 (GPa)
	Poisson's ratio	0.3

Where σ is the total stress. σ^e is the hyper-elastic stress component of Ogden material while σ^v is the added viscoelastic stress component and $G(t)$ is the relaxation function presented by the Prony series:

$$G(t) = \sum_{i=1}^n G_i e^{-\beta_i t} \quad (6)$$

Where G_i is a sequence of instantaneous shear module and β_i is a sequence of decay constants. This model is effectively a Maxwell fluid that consists of a dampers and springs in series. The viscoelastic behavior is optional and an arbitrary number of terms may be used. The parameters were shown in Table 3. Parameter fitting for each material was conducted using MATLAB code via the methodologies described by Ogden et al. (for Ogden material) and Park and Kim(for Prony series)^{[32][33]}.

The deformation was mainly suffered by muscle belly during the tensile tests because the stiffness of the tendon was far greater than the muscle belly. Thus the viscoelastic characteristic of tendon was not taken into account and the material of tendon was defined as linear elastic material with parameters shown in Table 3.

3 Kinematical Validation

3.1 Boundary Condition

The New HBM Head-Neck FE model was validated through the volunteer tests in 7g lateral impacts conducted at the Naval Biodynamics Laboratory (NBDL)^{[34][35]}. The volunteers (young and well trained marines) in the tests were seated in an upright position on a rigid seat mounted on a HYGE accelerator and exposed to short duration accelerations simulating lateral collisions. Accelerometers and photographic targets were mounted to the subject and used to monitor the resulting three-dimensional motions of the head and T1. Detailed description of the instrumentation and test methods were provided in the research of CL Ewing^{[34][35]}.

To simulate the validation, the horizontal T1-velocity (shown in Figure 7) referring from the recorded results of NBDL experiments tests was used as the input to the New HBM Head-Neck FE model. In the simulation, the horizontal T1-velocity was loaded on the topside node of the T1 vertebra along the lateral direction. The thorax model and the skull model were set rigid, and the thorax was allowed to translate in y direction and rotate about x axis only. Contacts functions between muscles, muscle and bone, bones were defined.

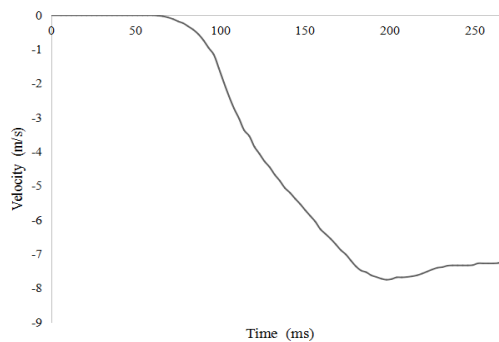


Figure 7. Horizontal T1-velocity in lateral collision

The active contracting forces modeling muscle activation were triggered by $A(t)$ -time history of muscle activation. Referring to studies conducted by MJ Horst et al^[12], the muscles were not immediately activated at the time of the collision simulation. Instead, It followed as:

$$t_{act} = t_{trigger} + t_{reflex} , \quad (7)$$

Where $t_{trigger}$ is defined as a certain sensory threshold time, t_{reflex} is a neural reflex time. The muscle activation dynamics was considered as the step-response to two linear first-order systems in series, describing the excitation and

activation dynamics. The two constants throughout the study were set 60 ms and 27 ms for $t_{trigger}$ and t_{reflex} respectively by the methods referred from the study conducted by MJ Horst et al. [12]. The muscles activation parameters: the maximum activation level (Act_{max}) and the time reaching the maximum activation level (t_{peak}) as well as the time reaching the end of activation (t_{end}), were shown in Table 4.

Table 4. Muscle activations applied to the new HBM head-neck FE model

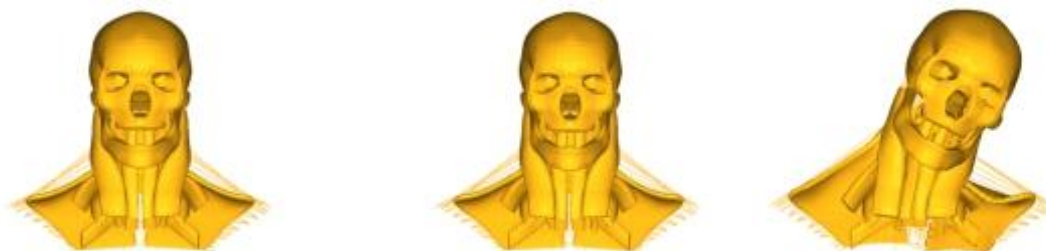
Impact direction	Muscle	Act_{max}	t_{peak} (ms)	t_{end} (ms)
Lateral	Longus colli, Hyoid muscles	0.8	180	End
	Contralateral muscles	0.6	180	230
	Ipsilateral SCM And Scalenus	0.95	250	End
	Ipsilateral others	0.75	250	End

Experimental and numerical studies [36] showed that the kinematics responses between Post Mortem Human Subject (PMHS) and volunteers were of great divergence since the mechanical properties of soft human tissues changed rapidly after the death of human being and the muscle activation was missing. By way of illustration, G.P Siegmund et al clarified the point that the activation of neck muscles was capable of generating forces that can alter head and neck kinematics responses [8]. To validate the New HBM-Head-Neck FE model, simulations with and without muscle activation were performed up to 300ms and the kinematics responses were measured. Then the results were compared with the experimental corridors.

3.2 Validation Results

The overall kinematics responses of the active New HBM-Head-Neck FE model after a lateral collision simulation was shown in Figure 8.

From 0 ms to 90ms, the model was in a static equilibrium state. Beyond this period T1 began to drive the cervical vertebra C2-C7 and the lower part of the cervical muscles moving rightward. Due to the inertia effect, the head and the C1 had no movement with respect to the initial space until 115ms. From 120ms to 180ms, the whole cervical spine was in an extended state and bended as a 'C' shape when the head reached its maximum rotation angle. During the period of 190ms to 270ms, the head and neck gradually rebounded under the traction force of cervical muscles and backed to the initial position at 270ms.



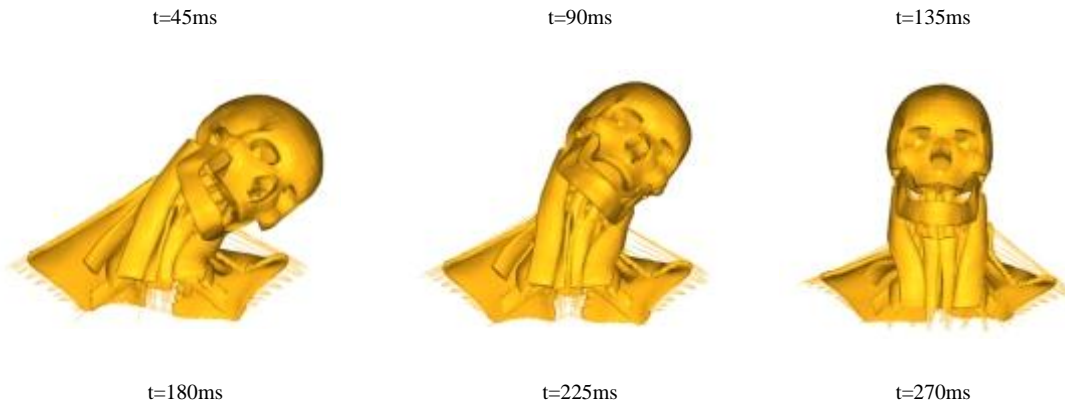


Figure 8. Movement of head-neck in Lateral impact

The position of the head was largely dominated by the head rotational angle and the head horizontal displacement during the simulation progress. Meanwhile, the speed change of the head movement was reflected by the head horizontal acceleration, which was an important parameter for the stability of the head movement. The head rotational angle, head horizontal displacement and head horizontal acceleration versus time, both passive and active, were shown in Figure 9. Also, the responses were in comparison with that of the HBM-Head-Neck Model II.

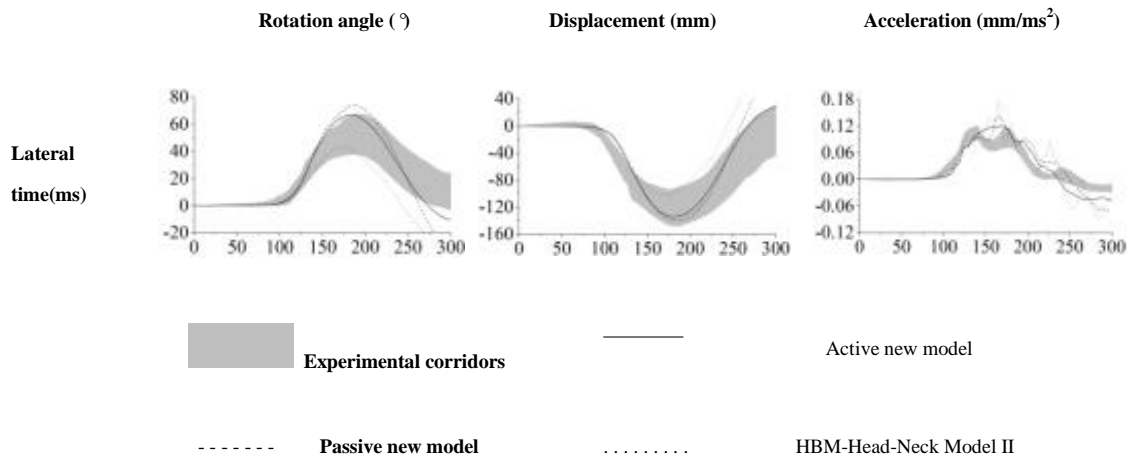


Figure 9. Head relative T1 kinematics responses for the numerical simulations with and without activation and the volunteer experimental corridors for lateral 7g impacts

With respect to the discrete model (HBM-Head-Neck Model II), the head rotation curve, the horizontal displacement curve and the head acceleration curve were in poor agreement with the experimental corridors. These mainly embodied in: Peak time for maximum value appeared in advance, head rebounded too fast and over-rebounded. Still, the acceleration curve contained obvious sharp fluctuations especially after 150ms.

In terms of the passive new model (passive New HBM-Head-Neck Model), only a few time periods of rotation angle and head displacement curves were within the experimental corridors. Meanwhile, the peak value of head displacement

ment was higher than the active one (active New HBM-Head-Neck Model) and the head rebounded faster. The acceleration curve of the passive model was consistent with the active one whereas the middle part was not and the peak acceleration value was much higher.

In contrast to the passive new model, the head rotation angle and the head displacement curves of the active one were closer to the upper limit of the experimental corridors, and most part of each curve lies within or near the experimentally defined corridors. Still, the peak value points were within the corridors, and the head horizontal acceleration curves shared the same trend with the corridors except the middle part.

4 Discussion

The present study focused on developing a human neck muscles FE model and integrating its geometric model into the HBM Head-Neck FE model as well as validating the combined model through volunteer tests by performing lateral collision simulations. The findings explained that the responses of the New HBM Head-Neck FE model were consistent with the experimental corridors.

The New HBM Head-Neck FE model developed (both passive and active) in the study increased the biofidelity enormously when comparing with the HBM-Head-Neck Model II. As can be seen from Figure 9, in lateral simulation, the responses curves of the HBM-Head-Neck Model II were in less reasonable agreement with the experimental corridors when contrasting with the New HBM Head-Neck FE model. Also, the acceleration curve displayed obvious oscillations especially after 150ms. These defects restricted the research application of HBM-Head-Neck Model II and limited its effectiveness to 0-150ms scope. Regarding the New HBM-Head-Neck Model, it cast aside the defects of HBM-Head-Neck Model II to some extent. During the lateral simulation, the responses of the New HBM-Head-Neck model were well in line with responses of experimental tests and displayed no oscillatory behavior. Meanwhile, due to the adding of hyoid and trachea, the model was more accurate with biofidelity much improved.

The biofidelity within the New HBM Head-Neck FE model in lateral collision may prove challenging to improve due to the structure of the model and the parameters of muscles. The difference of crest between acceleration response curve to the New HBM Head-Neck FE model and experimental data may result from the simplification of intervertebral disc, the gaps between neck muscles as well as the preload lack of the soft tissues. Meanwhile, the result that the response of head rotation angle rebounded faster than the experimental data may stem from the extra stiffness brought by the passive muscles and tissues, which indicated that the studies of parameters of muscles and tissues may need to be further undertaken.

By comparing the responses of passive New HBM-Head-Neck model with active New HBM-Head-Neck model, the study demonstrated that the activation of neck muscles produced enormous effects on the human head neck kinematics responses. It was analyzed that the activation of neck muscles played a positive role significantly in reducing the peak head acceleration, which was supported to lower the risk of head-neck injury in lateral collision. While owing to the lack of data on volunteer neck activity, the muscle activation curves during the validation process were adjusted by meeting the dynamic response requirements, which was an estimate that may not be sufficient enough to reflect the real response of volunteers in lateral collision. To improve the biofidelity of FE model and obtain better understanding of real response of human beings in lateral impacts, studies on the activity of muscles were therefore recommended.

So far, however, there has been a little discussion about the age effects on the activation of muscle while the effects were ignored in this study. Research conducted by Wang H et al found that the structural/compositional properties of skeletal muscle changed with age^[39], which suggested the necessity to apply the present new model in studying age effects through adjusting various parameters in material definition.

In general, the New HBM Head-Neck FE model had a good biofidelity in lateral collision, which can meet the requirements of studying the response of human head neck and the analysis of injury mechanism.

5 Conclusion

The following conclusions can be drawn from this study.

- (1) The New HBM Head-Neck FE model had a good biofidelity in lateral collision and was able to be used for future research.
- (2) The activation of neck muscles played a positive role significantly in reducing the risk of head-neck injury in lateral collisions.
- (3) To improve the biofidelity of the New HBM Head-Neck FE model, the structure of the model, the parameters of muscles as well as the muscle activity needed to be further studied.
- (4) It was necessary to apply the present model in studying age effects on the activation of neck muscles through adjusting various parameters in material definition.

References

- [1] Morris A, Hassan A, Mackay M, et al. Head injuries in lateral impact collisions.[J]. Accident; analysis and prevention, 1993, 27(6):749-56.
- [2] Erbulut D U. Biomechanics of neck injuries resulting from rear-end vehicle collisions.[J]. Turkish Neurosurgery, 2014, 24(4):466-70.
- [3] Dauvilliers F, Bendjellal F, Weiss M, et al. Development of a Finite Element Model of the Neck[C]// Stapp Car Crash Conference. 1994.
- [4] Jost R, Nurick G N. Development of a finite element model of the human neck subjected to high g-level lateral deceleration[J]. International Journal of Crashworthiness, 2000, 5(3):259-270.
- [5] Ejima S, Ono K, Kaneoka K, et al. Development and validation of the human neck muscle model under impact loading[C]// 2005.
- [6] Frechede B, Bertholon N, Saillant G, et al. Finite element model of the human neck during omni-directional impacts. Part II: relation between cervical curvature and risk of injury.[J]. Computer Methods in Biomechanics & Biomedical Engineering, 2006, 9(6):379-86.
- [7] Meyer F, Bourdet N, Deck C, et al. Human Neck Finite Element Model Development and Validation against Original Experimental Data.[J]. Stapp Car Crash Journal, 2004, 48:177-206.
- [8] Siegmund G P, Brault J R. Role of cervical muscles during whiplash[J]. Frontiers in whiplash trauma: clinical and biomechanical. IOS Press, Washington DC, 2000: 295-320.
- [9] Iwamoto M, Kisanuki Y, Watanabe I, et al. Development of a finite element model of the total human model for safety (THUMS) and application to injury reconstruction[C]// PROCEEDINGS OF THE INTERNATIONAL IRCOBI CONFERENCE. 2002.
- [10] Iwamoto M, Nakahira Y. A preliminary study to investigate muscular effects for pedestrian kinematics and injuries using active THUMS[C]// 2014.
- [11] Gayzik F S, Moreno D P, Pavalle N A, et al. Development of the global human body models consortium mid-sized male full body model[J]. Injury Biomechanics Research, 2011: 39-12.
- [12] Mj H V D, Mj H V D. Human head neck response in frontal, lateral and rear end impact loading : modelling and validation[J]. Knowledge & Process Management, 2002.
- [13] Fan L I, Honggeng L I, Wei H U, et al. SIMULATION OF MUSCLE ACTIVATION WITH COUPLED NONLINEAR FE MODELS[J]. Journal of Mechanics in Medicine & Biology, 2016.
- [14] Myers B S, Woolley C T, Slotter T L, et al. The influence of strain rate on the passive and stimulated engineering stress--large strain behavior of the rabbit tibialis anterior muscle.[J]. Journal of Biomechanical Engineering, 1998, 120(1):126-32.
- [15] Myers B S. ON THE STRUCTURAL AND MATERIAL PROPERTIES OF MAMMALIAN SKELETAL MUSCLE AND ITS RELEVANCE TO HUMAN CERVICAL IMPACT DYNAMICS[C]// Stapp Car Crash Conference. 1995.
- [16] Yang J, Yao J. Development and Validation of a Human Neck FE Model in Impact Loading Condition[J]. Journal of Hunan University, 2003, 30(4):40-46.
- [17] Kuang Y J, Wei X U, Ming W X. Development and Validation of a Head-Neck Finite Element Model for the Study of Neck Dynamic Responses in Car Impacts[J]. Journal of Hunan University, 2005.
- [18] Xu Wei. Finite Element Modeling of Head-Neck Biomechanical Responses of Occupant in Vehicle Crashes. Master thesis, Hunan University, 2004.
- [19] Fang W, Yang J, Li G. FINITE ELEMENT ANALYSIS OF HUMAN RIB FRACTURE UNDER VARIOUS IMPACT LOADING CONDITIONS[J]. Lixue Xuebao/chinese Journal of Theoretical & Applied Mechanics, 2014, 46(2):300-307.
- [20] Wang F, Xiao Z, Wan X, et al. FE Modeling of the Human Neck Responses in Low-Speed Car Collisions[M]// 6th World Congress of Biomechanics (WCB 2010). August 1-6, 2010 Singapore. Springer Berlin Heidelberg, 2010:513-516.
- [21] Wang F, Yang J, Li G. Finite element analysis on human thorax responses under quasi-static and dynamic loading[J]. Qiche Gongcheng/automotive Engineering, 2014, 36(2):189-150.
- [22] Li F, Laville A, Bonneau D, et al. Study on cervical muscle volume by means of three-dimensional reconstruction.[J]. Journal of Magnetic Resonance Imaging, 2014, 39(6):1411-6.
- [23] E. Jolivet, E. Daguët, V. Pomeroy, et al. Volumic patient-specific reconstruction of muscular system based on a reduced dataset of medical images[J]. Computer Methods in Biomechanics & Biomedical Engineering, 2008, 11(3):281-290.
- [24] Van Ee C A, Nightingale R W, Camacho D L, et al. Tensile properties of the human muscular and ligamentous cervical spine.[J]. Stapp Car Crash Journal, 2000, 44:85-102.
- [25] Goel V K, Liu Y K, Clark C R. Quantitative geometry of the muscular origins and insertions of the human head and neck[J]. Mechanisms of Head and Spine Trauma. Goshen, NY: Aloray: NY, 1986.

- [26] Kamibayashi L K, Richmond F J. Morphometry of human neck muscles.[J]. Spine, 1998, 23(12):1314-23.
- [27] Winters J M, Stark L. Analysis of fundamental human movement patterns through the use of in-depth antagonistic muscle models.[J]. Biomedical Engineering, IEEE Transactions on, 1985, BME-32(10):826-839.
- [28] Winters J M, Stark L. Estimated mechanical properties of synergistic muscles involved in movements of a variety of human joints.[J]. Journal of Biomechanics, 1988, 21(12):1027-41.
- [29] Winters J M. Hill-Based Muscle Models: A Systems Engineering Perspective[M]// Multiple Muscle Systems. 1990:69-93.
- [30] Zajac F E. Muscle and tendon: properties, models, scaling, and application to biomechanics and motor control.[J]. Critical Reviews in Biomedical Engineering, 1989, 17(4):359-411.
- [31] Hall-quist J. LS-DYNA Theory manual, Livermore software technology corporation, 2006[J]. Reproduced with permission of the copyright owner. Further reproduction prohibited without permission.
- [32] Ogden R W, Saccomandi G, Sgura I. Fitting hyperelastic models to experimental data[J]. Computational Mechanics, 2004, 34(6):484-502.
- [33] Park S W, Kim Y R. Fitting Prony-Series Viscoelastic Models with Power-Law Presmoothing[J]. Journal of Materials in Civil Engineering, 2001, 13(1):26-32.
- [34] Ewing C L, Thomas D J, Lustick L, et al. DYNAMIC RESPONSE OF HUMAN AND PRIMATE HEAD AND NECK TO +GY IMPACT ACCELERATION[J]. Equipment, 1978.
- [35] Ewing C L, Thomas D J. Human Head and Neck Response to Impact Acceleration[J]. Human Head & Neck Response to Impact Acceleration, 1972.
- [36] Ewing C, Thomas D, Lustick L, et al. Effect of duration, rate of onset and peak sled acceleration on the dynamic response of the human head and neck[J]. 1976.
- [37] Fice J B, Cronin D S. Investigation of whiplash injuries in the upper cervical spine using a detailed neck model.[J]. Journal of Biomechanics, 2012, 45(45):1098-102.
- [38] Wismans J, Philippens M, Oorschot E V, et al. Comparison of human volunteer and cadaver head-neck response in frontal flexion[M]// A treatise on differential equations /. Macmillan and co. 1988:1-13.
- [39] Wang H, Meunier B, Goh K L, et al. Age-Related Feature Extraction on Mouse Skeletal Muscle: Data Mining Approach[J]. Journal of Medical Imaging & Health Informatics, 2012, 2(4):386-392.
- [40] Feller L, Kleinbach C, Fehr J, et al. Incorporating Muscle Activation Dynamics into the Global Human Body Model[J].